Available online at www.sciencedirect.com
SCIENCE DIRECT
Polymer 47 (2006) 5025–5034
polymer
www.elsevier.com/locate/polymer

Determination of reactivity ratios and swelling characteristics of 'stimuli' responsive copolymers of *N*-acryloyl-*N*′-ethyl piperazine and MMA

G. Roshan Deen *, L.H. Gan

Chemistry Division, School of Natural Science, Nanyang Technological University, 1 Nanyang walk, Singapore, Singapore

Received 3 January 2006; received in revised form 20 March 2006; accepted 4 May 2006
Available online 30 May 2006

Abstract

'Stimuli' responsive copolymers of *N*-acryloyl-*N*′-ethyl piperazine (AcrNEP) and methyl methacrylate (MMA) were synthesized by free radical solution polymerization. The copolymers were analyzed as thin films by FTIR spectroscopy. The monomer reactivity ratios were determined by linearization methods of Fineman–Ross (F–R) and Kelen–Tüdös (K–T) giving the results r_1 (AcrNEP) = 0.58 and r_2 (MMA) = 0.91 by the F–R method and $r_1 = 0.72$ and $r_2 = 1.08$ by the K–T method. The latter r values in turn yielded $Q = 0.59$ and $e = -0.12$ for AcrNEP. Crosslinked copolymer hydrogels of AcrNEP and MMA with various compositions were prepared in bulk and solution by photo-initiated free-radical polymerization. The gels were dual responsive to pH and temperature. The response to pH was reversible with a response time of 100 min with good reversibility and with no loss in swelling capacity. Water sorption of the gels was investigated gravimetrically and the collective diffusion coefficients were determined at 10, 25, and 50 °C. The water sorption of the gels in water was Fickian. The temperature dependence of the equilibrium water content was studied by the Gibbs–Helmholtz equation. The enthalpy of mixing decreased with an increase in the hydrophilic content (AcrNEP) of the gel. Other parameters such as type and amount of crosslinker, preparative conditions, nature of buffers, and salts were found to influence the swelling behavior.

Keywords: *N*-acryloyl-*N*′-ethyl piperazine; Hydrogels; Water sorption

1. Introduction

In recent years, new research emphasis has been directed towards integrating multiple functions into polymeric materials. Among these new advances in materials science are functional polymers with structural designs intended to produce a specific polymer function. 'Stimuli' responsive polymers are polymers, which change their physical properties in response to external stimuli such as pH, temperature, electric field, illumination, magnetic field, etc. [1–6]. The potential responses to these stimuli can be changes in phase, shape, volume, and optical properties and these materials find applications in controlled drug delivery systems, skin care products, enzyme immobilizations, chemical sensors etc [7–11]. These types of polymers are soluble in water but undergo phase transition in response to temperature changes and separates into two phases. This temperature is termed the lower critical solution temperature (LCST) and is a result of disruption of hydrogen bonds between the polymer chains and solvent molecules.

When polymers of these kind are crosslinked with suitable crosslinking agents it results in the formation of hydrogels. For gels to be capable of responding strongly to slight changes in the external medium, a first-order phase transition accompanied by a sharp decrease in the specific volume of the macromolecule should take place. This has been associated with a critical transition temperature similar to LCST of uncrosslinked polymers [9–13]. In copolymeric systems the swelling process can be controlled by the introduction of the appropriate amount of a second monomer with hydrophobic character. The hydration degree and the swelling kinetics of such systems are controlled mainly by the crosslinking density and chemical composition and distribution of hydrophobic monomer units along the polymer chain [14].

In this report, we present the copolymerization behavior of AcrNEP and MMA in solution, and the determination of monomer reactivity ratios. Preparation of hydrogels based on these systems, their response to various stimuli, and their water sorption characteristics are also described. In this system,

* Corresponding author. Address: Department of Chemistry, University of Aarhus, Langelandsgade 140, Aarhus C, Denmark. Tel.: +45 8942 3929; fax: +45 8619 6199.
E-mail address: roshan@chem.au.dk (G.R. Deen).

0032-3861/$ - see front matter © 2006 Elsevier Ltd. All rights reserved.
doi:10.1016/j.polymer.2006.05.003

AcrNEP is hydrophilic and MMA is incorporated as the hydrophobic monomer to achieve the hydrophilic–hydrophobic balance.

2. Experimental

2.1. Materials

Acryloyl chloride (Fluka), ethylene glycoldimethacrylate (EGDMA) (Fluka), and methyl methacrylate (MMA) (Merck) were distilled under reduced pressure and stored in a refrigerator. *N*-ethyl piperazine (Aldrich) was stored over molecular sieves (3 Å) prior to use. Azobisisobutyronitrile (AIBN) (TCI) was recrystallized in methanol. 1,1-Dimethoxy-1-phenyl acetophenone (DMPA) (Aldrich) was used as received. 1,4-Dioxane (Merck), and tetrahydrofuran (THF) (Baker) were refluxed with metallic sodium for 3 h and distilled under nitrogen. All other chemicals were used as received. Buffer solutions of Na_2HPO_4–NaH_2PO_4 were prepared by adjusting 0.1 M NaH_2PO_4 solution with Na_2HPO_4 to the desired pH. Double distilled Milli-Q water (Barnstead Model D4755, USA) was used for all sample preparations.

The monomer *N*-acryloyl-*N*′-ethyl piperazine (AcrNEP) was synthesized by following the procedure described previously [15,16].

2.2. Synthesis of statistical copolymers of AcrNEP with MMA

Linear copolymers of AcrNEP and MMA with various monomer ratios were prepared in solution. The synthesis of linear copolymer BCP-A is described as follows: AcrNEP (0.7 mmol) MMA (9.3 mmol), and AIBN (0.5 wt%) were dissolved in 20 ml of freshly distilled 1,4-dioxane. The reactants were degassed three times by freeze–thaw cycle and the flask was sealed under vacuum. Polymerization was carried out at 75 °C for about 30 min and the content of the flask was poured into 400 ml of diethyl ether to isolate the copolymer. The copolymer was purified by re-precipitation and dried in vacuum at 50 °C for 1 day. For all samples the polymer conversion was limited to 10%.

2.3. Synthesis of crosslinked copolymer networks of AcrNEP

Crosslinked copolymer hydrogels with various amount of crosslinker were prepared and the procedure for a gel with 2 wt% crosslinker is described. AcrNEP (0.66 g, 3.91 mmol), MMA (0.35 g, 3.43 mmol), EGDMA (2 wt%) and DMPA (0.3 wt%) were mixed in a glass ampoule. The content was degassed by bubbling dry nitrogen for about 10 min and the ampoule was sealed. The sealed ampoule was then sonicated for 5 min to expel any gas bubbles. Polymerization was carried out in a photochemical reactor by UV irradiation ($\lambda > 300$ nm) for 30 min. The clear transparent polymer was recovered and soaked in diethyl ether for 2 weeks to remove any unreacted monomers (ether was replenished each day). The polymer was then cut into small discs of diameter (ca. 1.5 mm) and dried to constant weight in vacuum. The monomer feed compositions for the preparation of the gels and their appearance after polymerization is given in Table 1. The structure of the copolymer and crosslinker used in the preparation of the gels are shown in Fig. 1.

2.4. Determination of reactivity ratios

The composition of the copolymers were determined by infra-red spectral analysis on Perkin–Elmer (model 1725 X) FTIR spectrophotometer. The copolymers were analyzed as thin films on NaCl windows. The monomer reactivity ratios were determined by analyzing the relative intensities of the two carbonyl absorptions of the two monomers. In the cases where there was slight overlapping of the two absorptions, deconvolution treatment was first performed by the Perkin–Elmer IRDM software. The ratio of the monomer units in the copolymer was calculated from the following copolymer equation using known molar extinction coefficient of related systems [16].

$$\left[\frac{\text{MMA}}{\text{AcrNEP}}\right] = \frac{A_{\text{MMA}}}{A_{\text{AcrNEP}}} \times \frac{\varepsilon_{\text{AcrNEP}}}{\varepsilon_{\text{MMA}}} \tag{1}$$

where A and ε are the absorbance and molar extinction coefficient, respectively. The following ε values of 300 and 330 $dm^3\,mol^{-1}\,cm^{-1}$ for MMA and AcrNEP were used, respectively.

2.5. Equilibrium swelling studies

Gravimetric equilibrium swelling of the copolymer gels was studied to determine their sensitivity to pH, and temperature. For the study of the effect of pH on the swelling, sodium-acetate–acetic acid (pH 2.6–5.6) and sodium hydrogen phosphate–di-sodium hydrogen phosphate (pH 6.3–9.1) buffer

Table 1
Monomer feed composition for the preparation of hydrogels

Gel[a]	Feed compositions				Appearance after polymerization
	AcrNEP		MMA		
	(g)	(mmol)	(g)	(mmol)	
BG1(2)	0.6571	3.91	0.3452	3.43	Clear
BG2(2)	0.7672	4.57	0.2340	2.34	Clear
BG3(2)	0.8389	4.99	0.1619	1.52	Clear

[a] Values in parenthesis indicate the amount of crosslinker (wt%) used.

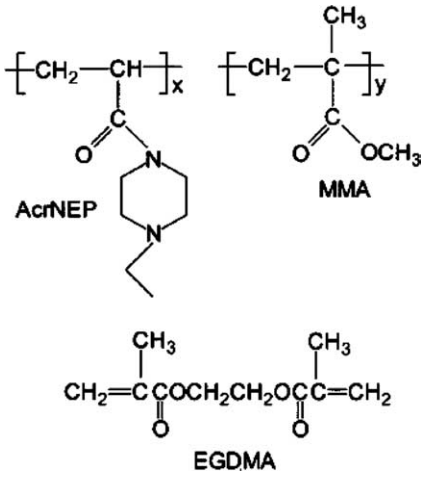

Fig. 1. Chemical structure of copolymer and crosslinking agents.

solutions were used. The gels were cut into small discs and immersed in respective buffer solutions in glass vials at 25 °C for 1 week. Each sample was then removed from the respective vials, tapped with a dampened Kim-wipe towel to remove the excess surface water and weighed. The dry weights were measured after desiccating the gels for 3 days under vacuum at 40 °C until constant dry weights were maintained. All the swelling experiments were performed in duplicate and the swelling ratio (by weight) was calculated as follows

$$\mathrm{SW} = \left(\frac{W_t - W_d}{W_d}\right) \tag{2}$$

where W_t and W_d are the wet weight and dry weight of the sample, respectively.

To study the effect of temperature on the swelling, the gels were immersed and equilibrated in deionized water at 25 °C for 2 days. The vials were in turn allowed to stand in a constant temperature bath set to a desired temperature. The swollen gel at each temperature of interest was allowed to equilibrate for 30 min before each measurement. The swelling ratio was calculated from Eq. (2).

2.6. Water sorption studies

The gel discs (ca. 0.15 g) were accurately weighed and placed in glass vials with 10 ml of distilled water. The vials were placed in a thermostated water-bath at the desired temperature. The water uptake W was calculated by measuring the weight gain of the sample at different times after carefully wiping the surface of the gels. The water uptake was calculated using the following expression

$$W = \frac{M_t - M_0}{M_0} \tag{3}$$

where M_0 is the weight of the dry sample and M_t is that of the sample at time t.

3. Results and discussions

3.1. Determination of monomer reactivity ratios

The monomer reactivity ratios were determined by analyzing the two carbonyl absorptions at around 1728 and 1636 cm^{-1} for the two monomer units namely MMA and AcrNEP, respectively. Fig. 2 shows the IR spectra of some of the copolymers and the compositions determined using Eq. (1) are given in Table 2. A plot of the mole fractions of AcrNEP in the copolymer (F_1) versus that in the feed (f_1) is shown in Fig. 3. It can be observed that the copolymers tend towards an almost ideal behavior. From the monomer feed ratios and the resultant copolymer compositions, the reactivity ratios of AcrNEP and MMA were evaluated by the linearization methods of Fineman–Ross (FR) [17] and Kelen–Tüdös (K–T) [18]. The FR equation is given as

$$\frac{f(F-1)}{F} = r_1\left(\frac{f^2}{F}\right) - r^2 \tag{4}$$

where subscript 1 denotes AcrNEP and subscript 2 denotes MMA, and $F = F_1/F_2$ and $f = f_1/f_2$. The FR plots can be made in two ways. In the first method called the FR1 method, $f(F-1)/F$ is plotted versus f^2/F, and then r_1 is the slope of the straight line and $-r_2$ the intercept. In the second method called the FR2 method, $(2F_1-1)(1-f_1)/(1-F_1)f_1$ is plotted versus $(1-f_1)^2F_1/(1-F_1)f^2$. In this plot, the slope gives $-r_2$ and the intercept gives r_1. However, the FR2 method is not often applied. The respective least-square plots are shown in Fig. 4(A) and 4(B), respectively. Straight lines with correlation factors of 0.9946 and 0.9896 were obtained for the FR1 and FR2 plots.

The reactivity ratios, r_1 and r_2 obtained from the FR1 plot were 0.58 ± 0.02 and 0.91 ± 0.07, respectively, while those obtained from FR2 plot were 0.38 ± 0.23 and 0.85 ± 0.04. A few comments can be added about the FR method. As observed from Fig. 4(A), in most cases, the FR straight line is plotted from several points gathered closely with one fairly isolated

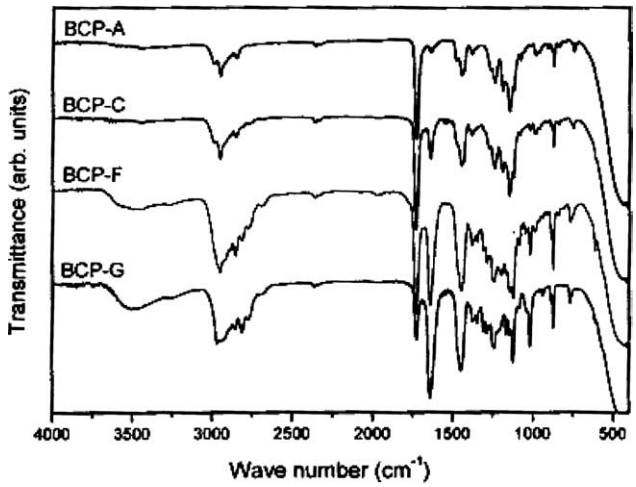

Fig. 2. FTIR spectra of linear copolymers of AcrNEP and MMA (film on NaCl window).

Table 2
Copolymer compositions determined by FTIR method

Copolymer	Feed (f) (mole fraction)		Conversion (%)	IR absorbance (cm^{-1})		Copolymer (F) (mole fraction)	
	AcrNEP (f_1)	MMA (f_2)		AcrNEP	MMA	AcrNEP (f_1)	MMA (f_2)
BCP-A	0.07	0.93	10.2	0.39	0.01	0.08	0.92
BCP-B	0.13	0.87	10.5	0.77	0.11	0.12	0.88
BCP-C	0.20	0.80	11.0	0.61	0.15	0.18	0.82
BCP-D	0.29	0.71	8.7	0.43	0.22	0.27	0.73
BCP-E	0.35	0.65	12.1	0.73	0.38	0.31	0.69
BCP-F	0.47	0.53	7.6	0.60	0.24	0.42	0.58
BCP-G	0.58	0.42	9.0	0.63	0.55	0.51	0.49
BCP-H	0.64	0.36	10.6	0.67	0.41	0.60	0.40
BCP-I	0.70	0.30	10.1	0.51	0.26	0.64	0.36
BCP-J	0.84	0.16	10.3	0.58	0.16	0.77	0.23

point. This last point corresponds to the highest value of f_1 in the FR1 method and the lowest one in FR2 method. The contribution from this point is vital for the determination of the slope of the straight line (r_1 for FR1, $-r_2$ for FR2). Since, high f_1 values are more representative of r_1 values and low ones of r_2 values [19] the FR1 method is more accurate for determining r_1 and FR2 method for calculating r_2.

The second linearization method to calculate the monomer reactivity ratios is that of Kelen–Tüdös according to the following equation

$$\eta = \left[r_1 + \left(\frac{r_2}{\alpha}\right)\right]\xi - \left[\frac{r_2}{\alpha}\right] \tag{5}$$

where η and ξ are functions of the molar ratios of the monomers in the copolymer and in the feed, α is any arbitrary denominator having any positive value, but so chosen as to give a more homogeneous distribution of data along the axis of η and ξ.

The values of r_1 and r_2 were calculated from the linear plot of η versus ξ. Thus, r_1 is the value of η when $\xi = 1$, and the intercept of the straight line $\eta = -r_2/\alpha$. The FR and KT parameters obtained for the copolymerization of AcrNEP and MMA are given in Table 3. The value of α was calculated as $\alpha = (H_{min} \times H_{max})^{1/2}$ by substituting the minimum and maximum value of H for an even distribution of the data points. H is defined as f^2/F. Thus, $(0.0647 \times 8.0993)^{1/2}$ gave a value of 0.7239 for α. The KT plot for the AcrNEP–MMA pair is shown in Fig. 5 from which the reactivity ratios, r_1 (AcrNEP) $= 0.72 \pm 0.07$ and r_2 (MMA) $= 1.08 \pm 0.04$ were obtained. The summary of the reactivity ratios obtained by the two linearization methods is given in Table 4.

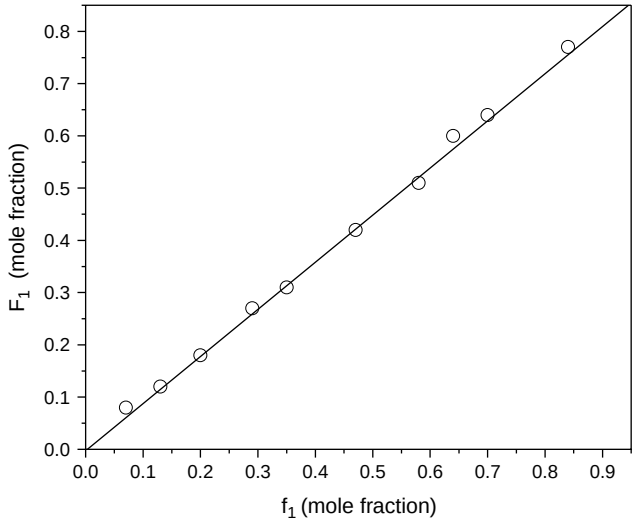

Fig. 3. Composition diagram for copolymerization of AcrNEP with MMA.

The difference in the reactivity ratios of AcrNEP and MMA obtained by the two methods is acceptable considering the inherent limitations of the methods. The value of r_2 is higher than r_1. The higher reactivity of MMA can be explained on the basis of π electron availability and the stability of the radical. In the case of AcrNEP the electron withdrawing carbonyl group decreases the electron density around the double bond, thus making it less susceptible for attack by free radicals. For MMA, the –I effect of the carbonyl is active, which reduces the reactivity. However, the hyperconjugation of the methyl group and the presence of a lone pair of electrons on the methoxy oxygen may have compensated for the polarization of the carbonyl. This renders the double bond more available for free radical attack and thus leads to higher reactivity [20].

The obtained value of $r_1 \times r_2$ indicates that the copolymer has a lower content of AcrNEP than the feed and show a random distribution of monomer units with tendency towards ideal behavior [16–20].

3.2. Comparison of calculated and experimental composition curves

Based on the values of r_1 and r_2 obtained from KT method ($r_1 = 0.72$) and ($r_2 = 1.08$), the composition diagram was obtained from the 'instantaneous copolymer composition equation' as,

$$F_1 = \frac{(r_1 f_1^2 + f_1 f_2)}{(r_1 f_1^2 + r_2 f_2^2 + 2 f_1 f_2)} \tag{6}$$

This was compared to the experimental data and the plot is shown in Fig. 6.

3.3. Statistical microstructure

The distribution of monomer sequences along the copolymer chain was calculated on the basis of terminal

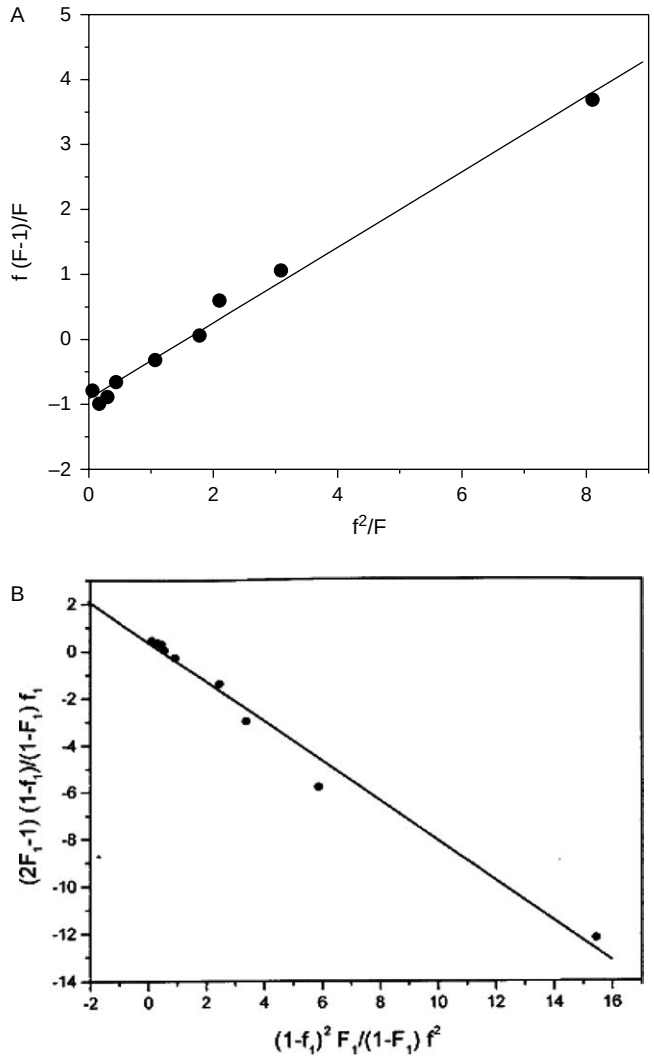

Fig. 4. (A) Fineman–Ross (FR1) plot for copolymerization of AcrNEP with MMA. (B) Fineman–Ross (FR2) plot for copolymerization of AcrNEP with MMA.

copolymerization model described by Igarashi [21]. This method calculates statistically the fractions AcrNEP–AcrNEP (M_1–M_1), MMA–MMA (M_2–M_2), and AcrNEP–MMA (M_1–M_2) units in the copolymers as a function of reactivity ratios and compositions. If X, Y, and Z are functions of M_1–M_1, M_2–M_2, and M_1–M_2 units in the copolymer then

$$X = \frac{\theta_1}{(\theta_1 + \theta_2 + \theta_3)} \tag{7}$$

$$Y = \frac{\theta_2}{(\theta_1 + \theta_2 + \theta_3)} \tag{8}$$

$$Z = \frac{\theta_3}{(\theta_1 + \theta_2 + \theta_3)} \tag{9}$$

where θ_1, θ_2, and θ_3 are the total number of M_1–M_1, M_2–M_2, and M_1–M_2 units in the copolymer. For a copolymer, P_{11} is defined as the probability for a monomer of the type M_1 to adjoin the other monomer of M_1. The same definition applies also to P_{22}. If $q = [(2F_1 - 1)^2 + 4r_1r_2F_1F_2]^{1/2}$, then

$$P_{11} = \frac{(2F_1 - 1 + q)}{(2F_1 + 2F_2 - 1 + q)} \tag{10}$$

$$P_{22} = \frac{2r_1r_2F_2}{(2r_1r_2F_2 + 2F_1 - 1 + q)} \tag{11}$$

where F_1 and F_2 are the mole fractions of M_1 and M_2 units in the copolymer and r_1 and r_2 are the reactivity ratios. X, Y, and Z are related to P_{11}, P_{22}, F_1 and F_2 as follows, $X \approx P_{11}F_1$, $Y \approx P_{22}F_2$, and $Z \approx (1 - P_{11})F_1 + 1(1 - P_{22})F_2$. By substituting Eqs. (10) and (11) into these equations X, Y, and Z can be obtained in terms of mole fractions. The results are plotted as triad fraction as a function of f_1 and is shown in Fig. 7. This result further supports the alternating tendency of the copolymers as determined earlier by the compositional and reactivity ratio studies. It can be observed from the triad fraction that the maximum alternation occurs approximately at 58 mol%. It is also evident that the triad fraction M_1–M_1 increases with increasing f_1, while triad fraction M_2–M_2 decreases with increasing f_1.

3.4. Calculation of Q and e values

The Q and e values for AcrNEP were calculated from the monomer reactivity ratios determined by the KT method using

Table 3
F–R and K–T parameters of the copolymers

Copolymer	$F = F_1/F_2$	$f = f_1/f_2$	FR1		KT	
			$G = f(F-1)/F$	$H = f^2/F$	$\eta = G/(\alpha + H)$	$\xi = H/(\alpha + H)$
BCP-A	0.09	0.07	−0.79	0.06	−1.00	−0.08
BCP-B	0.13	0.15	−0.99	0.17	−1.11	0.19
BCP-C	0.22	0.26	−0.89	0.30	−0.88	0.29
BCP-D	0.38	0.41	−0.66	0.44	−0.56	0.38
BCP-E	0.74	0.89	−0.32	1.07	−0.18	0.60
BCP-F	1.04	1.37	0.06	1.78	0.02	0.71
BCP-G	1.50	1.78	0.60	2.10	0.21	0.74
BCP-H	1.81	2.36	1.06	3.09	0.28	0.81
BCP-I	3.39	5.24	3.69	8.10	0.42	0.92

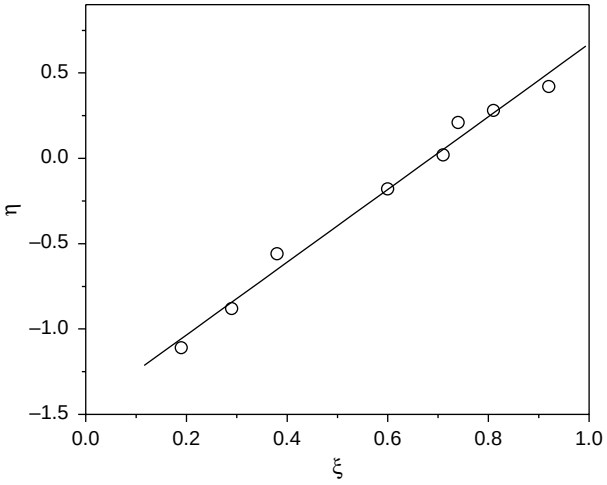

Fig. 5. Kelen–Tüdös plot for copolymerization.

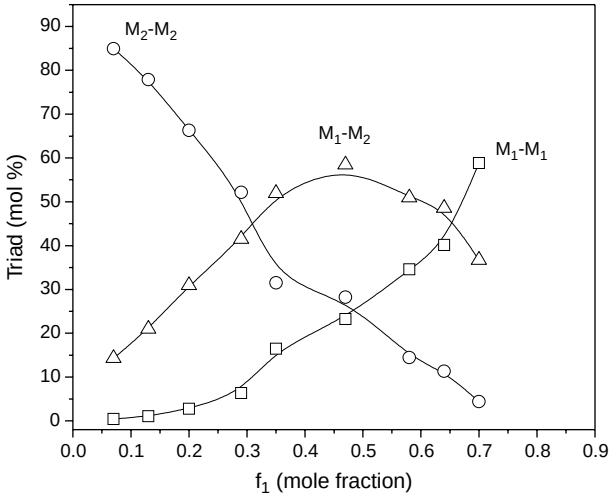

Fig. 7. Dependence of triad fractions on comonomer composition.

Table 4
Reactivity ratios determined by F–R and K–T methods

Method	Parameters		
	r_1	r_2	$r_1 \times r_2$
FR1	0.58±0.02	0.91±0.07	0.53±0.02
FR2	0.38±0.23	0.85±0.04	0.32±0.07
KT	0.72±0.07	1.08±0.04	0.32±0.46

the Alfrey–Price [22] equation

$$e_1 = e_2 \pm [-\ln r_1 r_2]^{1/2} \tag{12}$$

$$Q_1 = \left(\frac{Q_2}{r_2}\right) \exp -[e_2(e_2 - e_1)] \tag{13}$$

where Q and e are the reactivity and polarity of the monomer and r_1 and r_2 are the reactivity ratios. Using the values of r_1 and r_2 by the KT method and $Q=0.78$, $e=0.40$ for MMA [23], two sets of Q–e values were obtained for AcrNEP (i) $Q=0.89$, $e=0.91$ and (ii) $Q=0.59$, $e=-0.12$. The second set of value was chosen because these values compared reasonably well with $Q=0.56$, $e=-0.49$ for *N*-acryloyl-*N*′-methyl piperazine and *N*,*N*-dimethyl acrylamide [16].

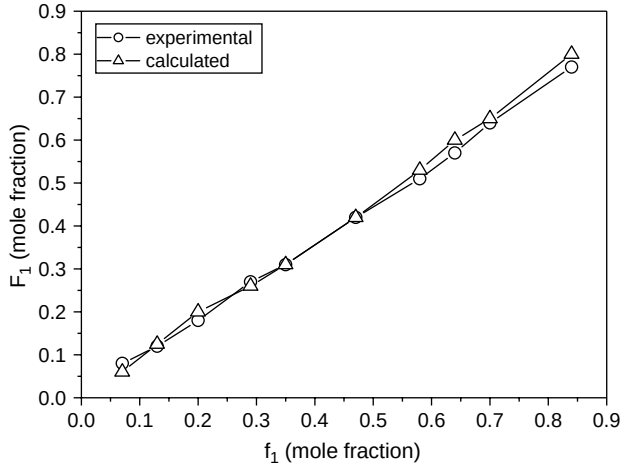

Fig. 6. Instantaneous copolymer composition curve.

3.5. Effect of pH on the swelling of gels prepared in solution

The effect of pH on the swelling of gels containing 2 wt% crosslinker was investigated and is shown in Fig. 8. The gels swelled extensively in acidic medium and de-swelled in neutral and alkaline media. A maximum swelling ratio of about 70 was observed for BG3(2) due to protonation of the tertiary amine groups, causing electrostatic repulsions. This leads to an osmotic pressure gradient within and outside the gel causing it to swell [24]. The pK_a of the basic nitrogen of this polymer was determined to be 4.58 by potentiometric titration [25], suggesting polyelectrolyte behavior [26]. It is further observed that with increase in the content of ionizable species in the gel (piperazine), the swelling ratio increased significantly. The swelling transition was gradual and such information is important for ionizable gels because they may have potential pharmaceutical applications.

3.6. Effect of preparation method on the swelling of gels

The method of gel preparation was found to have a profound effect on the swelling of the gel. Fig. 9 shows the effect of pH on the swelling of gels prepared by bulk polymerization. It can be seen that swelling is considerably low (by ∼10 times) compared to that exhibited by gels prepared in solution. This is attributed to additional crosslinking. Polymers prepared in bulk have high elastic constraint, which leads to lower swelling. Similar behavior has been reported for gels prepared from *N*,*N*-dimethylaminoethyl methacrylate and *n*-butyl acrylate prepared in bulk [24]. The gels prepared in solution are believed to contain porous network structures leading to higher swelling and sorption.

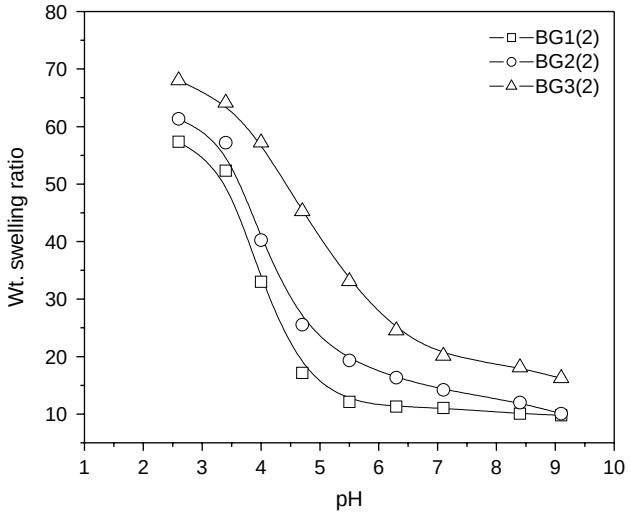

Fig. 8. Effect of pH on the swelling of gels at 25 °C (crosslinker content 2 wt%).

3.7. Effect of buffer type on swelling

The effect of nature of the buffer on the swelling of the gel (BG1(2)) prepared in bulk with 2 wt% EGDMA was investigated. The swelling ratio of the gel in acetate and citrus buffer of pH 3.6 at 25 °C were 7.13 and 2.71, respectively. The swelling was much lower in citrus buffer than in phosphate buffer. This can be explained based on the shift in the charge on the citrate counterions. Citrate buffer has three ionizable carboxylic acid groups, with pK_1 3.15, pK_2 4.78, and pK_3 6.40. At low pH, the citrate passes from a predominantly trianionic to dianionic and finally to monoionic state. These multivalent counterions are responsible for the observed lower swelling [27,28].

3.8. Effect of crosslinker content

The effect of crosslinker content on the pH dependent swelling of gels prepared in bulk was studied and is shown in Fig. 10. It followed a general trend by showing a decreased swelling with increase in crosslinker content. This is due to the formation of more rigid polymer networks at high crosslinker content, which affects the elastic modulus of the gels. The swelling ratio of BG1 gel decreased from 4.8 to about 2.5 between 2 and 6 wt% of crosslinker at pH 3. This is due to poor penetration of solvent owing to rigid gel networks.

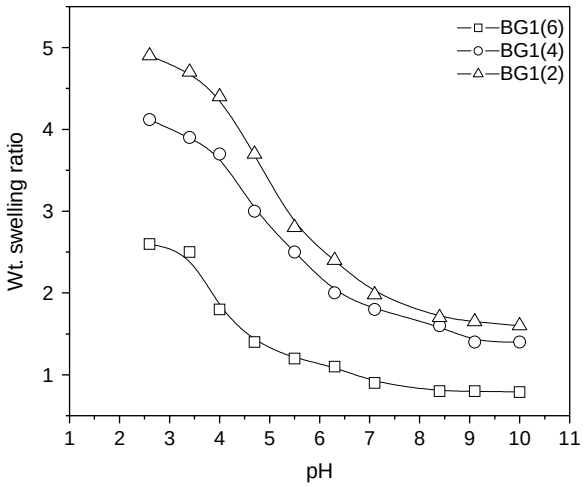

Fig. 10. Effect of crosslinker content on swelling in buffer solution of pH 2.6.

3.9. Effect of temperature

Fig. 11 shows the effect of temperature on the swelling of gel BG1(2) in water. This gel was prepared under bulk conditions. The gel swelled at low temperature and shrunk at high temperature with continuous transition. However, a slight manifestation around the LCST region of 33 °C (for the linear copolymer) was observed due to hydrophobic interactions of the polymer chains [6]. This gel transition temperature was close to that of poly(*N*-isopropyl acrylamide) (pNIPAAm), which shows a discontinuous transition at 32 °C [6,7,27]. The BG1(2) gel showed a rather continuous transition due to mild interactions among the hydrophobic groups. The effect of crosslinker on the temperature dependent swelling of the gels was also observed.

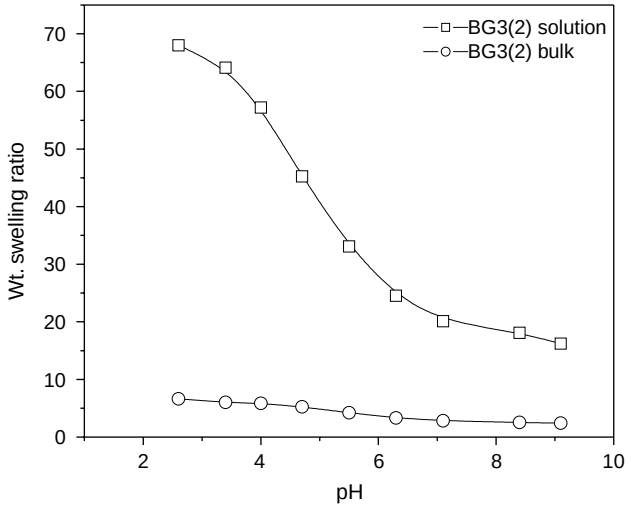

Fig. 9. Effect of preparative condition on the swelling of gels.

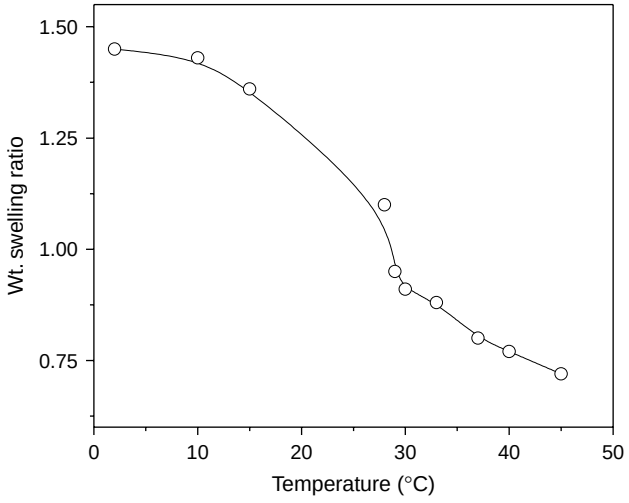

Fig. 11. Effect of temperature on swelling of gel in water.

Table 5
Swelling ratio of the hydrogel as a function of salt concentration

Gel	Wt swelling ratio					
	15 °C		25 °C		40 °C	
	0.05 M	3 M	0.05 M	3 M	0.05 M	3 M
BG1(2)	1.73	1.56	1.60	1.26	1.52	1.06

The swelling ratio decreased with increasing crosslinker content of the gel with a slight shift in the gel transition temperature.

3.10. Effect of NaCl on the swelling

Effect of simple salt like NaCl on the swelling of gel (bulk) BG1(2) in water (pH 7) as a function of temperature is given in Table 5. The swelling ratio decreased progressively with increasing NaCl concentration and temperature. The observed drop in the swelling with the salt concentration reflects a change in solubility or viscosity of the system. The LCST of the linear copolymers of this system described earlier [15] showed a linear dependence with NaCl concentration. In general, increasing the salt concentration decreases the solubility of the polymer in solution due to screening effects and similar behavior has been observed for poly(*N*-isopropylacrylamide) in salt solutions [29].

3.11. pH responsive swelling and deswelling profile

Fig. 12 shows the swelling profile of BG1(2) prepared in solution. The initially swollen gel in buffer solution of pH 2.6 was first placed in buffer solution of pH 7.1. The swollen gel gradually deswelled. It took about 100 min for the swelling ratio to reach a maximum value of about 55 and it took the same amount of time to deswell to a value of about 21. During this process, the fully protonated amine groups of the piperazine were mostly de-protonated leading to a decrease in ionization of the network. The re-swelling to fully swollen state from pH 7.1 to 2.6 followed almost the same response time. The average swelling ratio for three successive swelling kinetics were the same with an average response time of 100 min. Although the response time is high, it is demonstrated that reversibility between different states is possible with these types of gels that contain tertiary amine functions. The gel showed good reversibility with no decrease in swelling capacity.

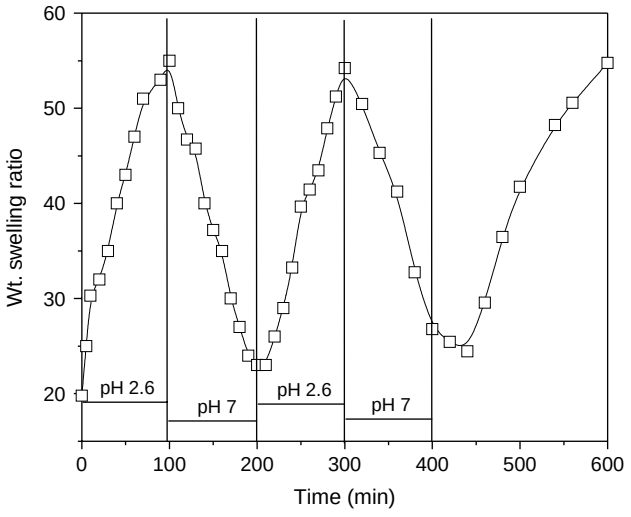

Fig. 12. Pulsatile pH responsive swelling and de-swelling profile of BG1(2) at 25 °C.

3.12. Water sorption kinetics

Fig. 13 shows the sorption isotherms for the bulk prepared gels in water at 25 °C. The water uptake increased with increasing hydrophilic comonomer of the gel, which is further reflected in the equilibrium water uptake W_∞, which is defined as the maximum swelling ratio. The values of equilibrium water uptake are given in Table 6. Two different processes describe the diffusion of solvent into the polymer matrix viz. the diffusion of solvent into the swollen matrix and advancement of the swollen–unswollen boundary as a result of polymer relaxation [30]. For sorption kinetics of the gels, the initial swelling data were fitted to the following equation in the range $M_t/M_\infty \leq 0.6$

$$\frac{M_t}{M_\infty} = kt^n \tag{14}$$

where M_t and M_∞ are the mass of water taken at time t and infinite time, respectively, k is a characteristic constant of the gel, and n is a characteristic exponent of the mode transport of the penetrate. The values of n and k were calculated from the slopes and intercepts of the plot of $\log(M_t/M_\infty)$ versus $\log(t)$. For Fickian kinetics in which the rate of diffusion of the solvent is rate limiting, n equals 0.5, while values of n between 0.5 and 1 indicate the contribution of non-Fickian processes such as polymer relaxation [28].

The collective diffusion coefficients of the gels were determined from the gradient of the plot of initial sorption rate versus square root of time in the range of M_t/M_∞ 0.6 as

$$\frac{M_t}{M_\infty} = \frac{4}{l}\left(\frac{Dt}{\pi}\right)^{1/2} = \frac{W_t}{W_\infty} \tag{15}$$

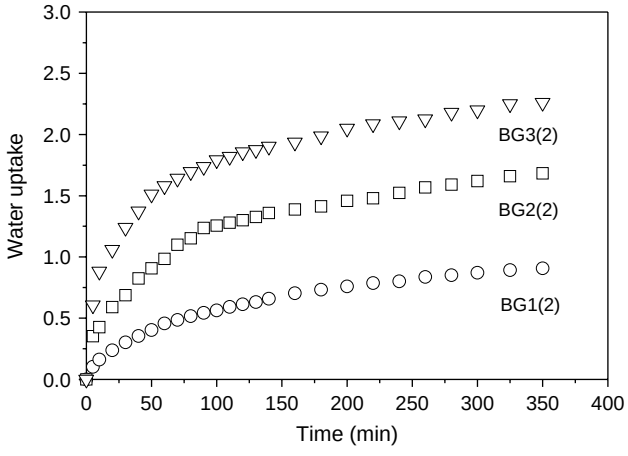

Fig. 13. Water sorption isotherm for gels in water (pH 7) at 25 °C.

Table 6
Equilibrium water uptake of the gels as a function of temperature

Gel	W_∞ (g water/g polymer)		
	10 °C	25 °C	50 °C
BG1(2)	1.5826	1.1027	0.8257
BG2(2)	1.6590	1.5295	1.1098
BG3(2)	1.8920	1.7123	1.3192

Table 7
Water sorption characteristics of the gels in water

Gel	T (°C)	l (cm)	n	k	$D\times10^7$ (cm^2 s^{-1})
BG1(2)	25	0.10	0.59	0.04	1.55
	50		0.55	0.006	3.42
BG2(2)	25	0.12	0.42	0.11	2.79
	50		0.46	0.005	6.01
BG3(2)	25	0.11	0.43	0.17	5.32
	50		0.61	0.07	8.31

where W_t and W_∞ are weight swelling ratios at time t and time infinity, respectively, t is the time and l is the initial thickness of the dry gel. The results are summarized in Table 7. It clearly indicates that diffusion of water in the gels follows Fickian behavior within the limits of experimental error. Schott [31] proposed an equation for describing polymers that has longer swelling times as

$$\frac{t}{W} = A + Bt \tag{16}$$

where W is the water uptake at time t, $B = 1/W_\infty$, the inverse of maximum swelling, and $A = 1/(\mathrm{d}W/\mathrm{d}t)_0$ the reciprocal initial swelling rate. It was further demonstrated by Schott that Eq. (16) implies second-order kinetics. Applying this equation to the swelling data, gave straight lines with good correlation coefficients. Fig. 14 shows the plot of reciprocal swelling rate versus time at 25 °C and similar results were obtained for water sorption at 10 and 50 °C.

With increasing hydrophilic content the values of D were found to increase due to greater penetration of water molecules into the gels. Since, these gels are ionizable at the tertiary amine functions, more complications arise because both solvent and ions must be transported into the gel in order to reach equilibrium. Therefore, under such conditions in addition to solvent diffusion and polymer relaxation, the other factors that contribute to the swelling are believed to be, ion diffusion and fixed charge group ionization. The understanding of the swelling process of these gels can be aided by Siegel's moving swelling front model [27].

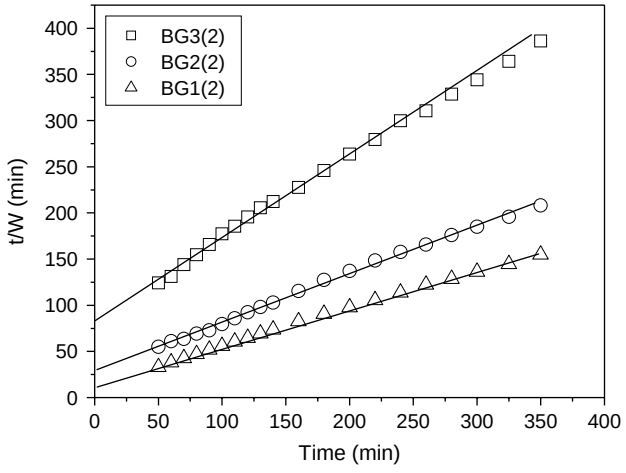

Fig. 14. Plots based on Schott's equation for gels (pH 7) at 25 °C.

At time equal to 0, the polymer disc immersed in a swelling medium is in its glassy state. The solvent and ions penetrate into the gel initiating the swelling process. During the process of swelling the polymer changes from its glassy state to rubbery state and becomes soft. Since, a certain threshold combination of solvent and ions must be present to initiate this transition, a front (swelling front) will appear separating the glassy core from the rubbery periphery. The rigid core constrains the swelling in the periphery allowing expansion only in the direction normal to the front. This constraint gives rise to a differential swelling stress, which can be a driving force for the movement of the swelling front. Owing to this, the moving fronts from the two opposing faces will meet. At this point, the swelling constraint diminishes whereby the differential swelling stress is released and swelling is permitted in all three dimensions leading to the observed acceleration. This is schematically illustrated in Fig. 15.

The enthalpy of mixing between the dry polymer and an infinite amount of water (ΔH_m) was calculated using the Gibbs–Helmholtz equation as,

$$\frac{\mathrm{d}\ln(W_\infty)}{\mathrm{d}(1/T)} = -\frac{\Delta H_\mathrm{m}}{R} \tag{17}$$

Plots of W_∞ versus reciprocal swelling temperature gave straight lines with positive slope (not shown). The positive slope indicates that the diffusion process is an exothermic mixing process and the values obtained in kJ mol^{-1} were, −12.13, −7.83, and −6.96 for BG1(2), BG2(2), and BG3(2), respectively. The absolute values of ΔH_m were dependent on the composition of the gels, and decreased with increasing hydrophilic content of the gels.

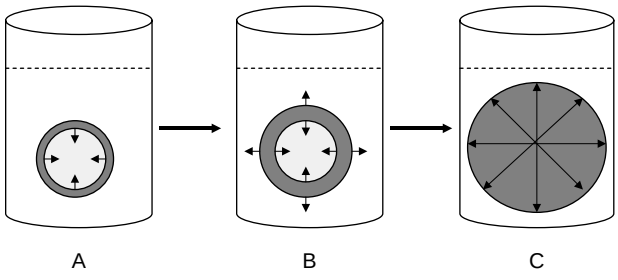

Fig. 15. Schematic illustration of moving swelling front in the swelling of gels; (A) appearance of a swelling front, (B) movement of swelling front and expansion of gel, (C) diminished swelling constraint followed by accelerated swelling.

4. Conclusions

'Stimuli' responsive linear copolymers of AcrNEP with MMA of various compositions were synthesized in solution by free radical polymerization using AIBN as initiator. The copolymer compositions were determined by FTIR spectroscopy. The reactivity ratios were determined by both the F–R and K–T methods, and the two methods yielded comparable results. It was found that AcrNEP was less reactive than MMA. The distribution of monomer sequence was calculated by Igarashi's model and maximum alternation of monomer segments was at 58 mol%.

Crosslinked copolymer hydrogels based on this system was responsive both to pH and temperature. Swelling and de-swelling profiles in pH 2.7 and 7 had a response time of about 100 min with excellent reversibility. No loss in swelling capacity was observed during repeated cycles. The extent of swelling of the gels could be designed to vary by changing the preparative conditions, amount and type of crosslinking agents etc. Water sorption of these gels followed Fickian behavior. This work has thus demonstrated that through proper choice of monomers and other experimental conditions, it is possible to tailor-make 'stimuli' responsive polymers with specific properties.

Acknowledgements

G.R.D. thanks the Nanyang Technological University for the research scholarship.

References

[1] Gonzalez N, Elvira C, San Román J. Macromolecules 2005;38:9298–303.
[2] Gan LH, Gan YY, Roshan Deen G. Macromolecules 2000;33:7893–7.
[3] Schild HG. Prog Polym Sci 1992;17:163–249.
[4] Chen G, Hoffman AS. Nature 1995;373:49.
[5] Frank S, Lauterbur P. Nature 1993;363:334.
[6] Galaev YI. Russ Chem Rev 1995;64:471.
[7] Qiu Y, Park K. Adv Drug Delivery Rev 2001;53:321–39.
[8] Galaev IY, Mattiason B. Trends Biotechnol 1999;17:335–40.
[9] Yhang J, Peppas NA. Macromolecules 2000;33:102–7.
[10] Tasdelen B, Kayaman AN, Guven O, Baysal B. Int J Pharm 2004;278:343–51.
[11] Hu Z, Lu X, Gao J. Adv Mater 2001;13:178–1712.
[12] Yoshida R, Sakai K, Okano T, Sakurai Y. J Biomater Sci Polym Ed 1994;6:585–98.
[13] Nath N, Chilkoti A. Adv Mater 2002;14:1243–7.
[14] Peniche C, Zaldivar B, Gallardo A, San Román J. J Appl Polym Sci 1994;54:959.
[15] Gan LH, Roshan Deen G, Loh XJ, Loh YY. Polymer 2001;42:65–9.
[16] Gan LH, Roshan Deen G, Gan YY. Eur Polym J 1998;34:33–6.
[17] Fineman M, Ross SD. J Polym Sci 1950;5:259.
[18] Kelen T, Tüdös F. J Macromol Sci Chem 1975;9:1.
[19] Malawska B, Goaille S. Pharmazie 1995;50:390.
[20] Nair CPR, Clouet G, Brossas J. J Polym Sci Polym chem Ed 1988;26:1791.
[21] Igarashi S. Polym Lett 1963;1:359.
[22] Alfrey Jr T, Price C. J Polym Sci 1963;A1:1137.
[23] Brandrup J, Immergut EH, editors. Polymer handbook. New York: Wiley; 1989.
[24] Siegel RA, Firestone BA. Macromolecules 1988;21:3254.
[25] Roshan Deen G. PhD, Dissertation, Nanyang Technological University 2000.
[26] Roshan Deen G, Gan LH, Tam KC. Polym Bull. Submitted for publication.
[27] Siegel RA. In: Dusek K, editor. Responsive gels: volume transitions I. Berlin: Springer; 1993.
[28] Krušić MK, Filipović J. Polymer 2006;47:148–55.
[29] Narang AS, Garg VC. J Ind chem Soc 1989;66:214.
[30] Peniche C, Cohen ME, Vázquez B, San Román J. Polymer 1997;38:5977.
[31] Schott HJ. Macromol Sci Phys 1992;B31:1.